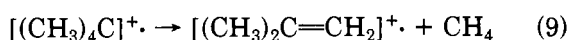
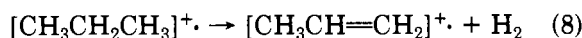


or  $\text{CH}_4$  to form the radical cation of an olefin, as in eq 8 and 9.<sup>62</sup>



We cite numerous recent publications on radical cations produced by the methods described above.<sup>71-92</sup>

We also note that the radiolytic method is now being applied for the study of biologically significant systems such as porphyrins.<sup>93-96</sup> Radical cations doubtlessly

(84) M. C. R. Symons, *J. Chem. Soc., Chem. Commun.* 869 (1982).

(85) D. N. R. Rao and M. C. R. Symons, *J. Chem. Soc., Perkin Trans. 2*, 135 (1983).

(86) H. Chandra and M. C. R. Symons, *J. Chem. Soc., Chem. Commun.* 29 (1983).

(87) A. Hasegawa and M. C. R. Symons, *J. Chem. Soc., Faraday Trans. 1*, 79, 93 (1983).

(88) M. Shiotani, Y. Nagata, M. Tasaki, J. Sohma, and T. Shida, *J. Phys. Chem.*, 87, 1170 (1983).

(89) K. Shimokoshi, J. Fujisawa, K. Nakamura, S. Sato, and T. Shida, *Chem. Phys. Lett.*, 99, 483 (1983).

(90) L. D. Snow, J. T. Wang, and F. Williams, *Chem. Phys. Lett.*, 100, 193 (1983).

(91) L. D. Snow and F. Williams, *Chem. Phys. Lett.*, 100, 198 (1983).

(92) D. Becker, K. Plante, and M. Sevilla, *J. Phys. Chem.*, 87, 1648 (1983).

play a key role in the photosynthetic process. Recognition of that role requires authentic spectral information.

### Concluding Remarks

In this Account the technique of the radiolytic production of radical ions in rigid organic media is explained in some detail and the usefulness of the spectroscopic data obtainable in this way is demonstrated. It is shown that the photolytic and radiolytic generation of ions are complementary in that the former technique gives very detailed spectral information while the latter is more generally applicable. The  $\text{CCl}_3\text{F}$  matrix is shown to be a seminal medium for the ESR study of various radical cations.

*E.H. and T.B. gratefully acknowledge generous support by the Swiss National Science Foundation. They thank Dr. Paul Suppan (Fribourg) for his help in the first stages of this Account.*

(93) H. Seki, S. Arai, T. Shida, and M. Imamura, *J. Am. Chem. Soc.*, 95, 3404 (1973).

(94) S. Konishi, M. Hoshino, and M. Imamura, *J. Phys. Chem.*, 86, 4537 (1982).

(95) M. Hoshino, S. Konishi, K. Ito, and M. Imamura, *Chem. Phys. Lett.*, 88, 138 (1982).

(96) D. N. R. Rao and M. C. R. Symons, *J. Chem. Soc., Faraday Trans. 1*, 79, 269 (1983).

## Structurally Complex Organic Ions: Thermochemistry and Noncovalent Interactions

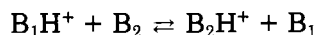
M. MEOT-NER (MAUTNER)

*Chemical Thermodynamics Division, Center for Chemical Physics, National Bureau of Standards, Washington, DC 20234*

*Received January 5, 1983 (Revised Manuscript Received January 3, 1984)*

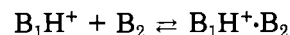
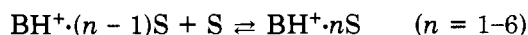
Protonated organic compounds play important roles in natural and technological systems. In many cases, the organic ions possess complex structures including such features as multiple functional groups, steric crowding, large size, and extensive conjugated  $\pi$ -electron systems. The effects of these features on the intrinsic, solvent-free thermochemical properties and interactions of the ions will be reviewed in this Account.

Mass spectrometric techniques developed in the last two decades can be used to obtain the thermochemistry of ions in the gas phase where solvent interactions are absent. Thus, gas-phase measurements can be applied to the proton-transfer equilibria between two gas-phase bases  $\text{B}_1$  and  $\text{B}_2$ :



These measurements yield the intrinsic solvent-free

relative basicities ( $\Delta G^\circ_{\text{proton transfer}}$ ) and relative proton affinities ( $\Delta H^\circ_{\text{proton transfer}}$ ) of organic molecules. Further, mass spectrometric measurements can also elucidate the details of ion-solvent interactions. Thus, we can measure in the gas phase the enthalpies and entropies of equilibria leading to the formation of the  $n$ -fold solvated cluster ions  $\text{BH}^+ \cdot n\text{S}$  and of dimer ions  $\text{B}_1\text{H}^+ \cdot \text{B}_2$ :



Gas-phase ion-molecule equilibria are usually measured by ion cyclotron resonance (ICR), flowing afterglow and pulsed high-pressure mass spectrometry (PHPMS). We use the latter technique, where, typically, reagents flow to the ion source as minor additives (0.01-10%) in a protonating ( $\text{CH}_4$ ,  $i\text{-C}_4\text{H}_{10}$ ,  $\text{H}_2\text{O}$ ) or ionizing ( $\text{C}_6\text{H}_6$ ,  $\text{CS}_2$ ,  $\text{N}_2$ ) gas. Solids can be introduced directly by a heated probe and the partial pressure measured by using ion-molecule kinetics; this makes the techniques applicable to refractory compounds such as polycyclic aromatics and nucleic bases. The total source pressure ranges from 0.1 to 2 torr, and the temperature is variable from 80 to 700 K. Ionic reactions are initiated by an electron pulse, and the change in ion signal intensities in the course of ion-molecule reactions

Michael Mautner was born in Budapest, Hungary. He moved to Israel (where he transliterated his name to Meot-Ner, "Hundreds of lights"). He received undergraduate training at the Hebrew University of Jerusalem. He obtained his M.Sc. at Georgetown University, worked as a research chemist at the New England Institute, Ridgefield, CT, and in 1975 obtained his Ph.D. at the Rockefeller University with Professor F. H. Field (1975). At Rockefeller University, he served as Assistant and then Associate Professor. He joined the Radiation Chemistry group at NBS in 1979. Research interests concern mass spectrometry, ion thermochemistry, ion-molecular reactions, and ion-neutral interactions and clustering, with applications to cosmochemistry and biophysics.

is followed to 2–4 ms. Equilibrium is indicated when the product/reagent ion intensities reach a constant ratio with reaction time. The technique is advantageous for our purposes, since the high pressure facilitates three-body complexing reactions. The wide temperature range allows the measurement of ion–neutral bonding energies from about 5 to 40 kcal mol<sup>-1</sup>, and the variable temperature allows the construction of van't Hoff plots from which enthalpy and entropy changes are obtained. The latter is of particular importance, since, as we shall observe, structural complexity often leads to substantial entropy effects.

A large body of gas-phase data on proton affinities of organic bases is now available, and analysis of this data reveals the effects of primary structural factors, such as polarizability, electronegativity, and orbital hybridization, as will be summarized below. Due to our interest in structural effects, we extended gas-phase measurements to organic ions that contain structural features. We observed that these structural features give rise to further interactions: intramolecular, partial, and multiple hydrogen bonding; steric entropy factors adverse to ion solvation; intramolecular and intermolecular charge resonance; and attractive van der Waals dispersion forces.

To identify effects of these secondary structural factors, comparisons with structurally simple ions are necessary. We therefore begin this Account with a brief discussion of effects of primary structural factors and solvation on the basicities ( $-\Delta G^\circ_{\text{protonation}}$ ) and proton affinities ( $-\Delta H^\circ_{\text{protonation}}$ ) of simple molecules. It must be noted at the outset that the separation of "primary" and "secondary" structural effects is somewhat arbitrary.

Early gas-phase measurements<sup>1,2</sup> revealed that the intrinsic proton affinities (PAs) of alkylamines vary in the gas phase in the order  $\text{NH}_3 > \text{CH}_3\text{NH}_2 > (\text{CH}_3)_2\text{NH} > (\text{CH}_3)_3\text{N}$  and span a range of 22 kcal mol<sup>-1</sup>. This is different from aqueous solution, where solvent effects compress the range of basicities in this series to less than 2 kcal mol<sup>-1</sup> and, in some cases, reverse the relative basicities.<sup>3</sup> Also, in the gas phase, PAs of the primary amines, alcohols, cyanides, and sulfides vary in the order  $\text{HX} < \text{CH}_3\text{X} < \text{C}_2\text{H}_5\text{X} < n\text{-C}_3\text{H}_7\text{X} \dots$  The regular sequences in the gas phase show a primary structure effect: polarizable groups increase the PA by delocalizing the charge on the protonated ions  $\text{RXH}^+$ . Another primary factor is the electronegativity and hybridization of the heteroatoms subject to proton attachment.<sup>4</sup> For example, for a given substituent group R, the proton affinities vary in the order  $\text{ROH} < \text{RCHO} < \text{RSH} < \text{RCN} < \text{RNH}_2$ . More quantitatively, correlations were found between PAs and lone pair of 1s ionization potentials of the functional groups.<sup>5,6</sup> The effects of these factors—polarizabilities, hybridization, and correlations with lone-pair or 1s ionization potentials—may be termed primary structure effects on proton affinities.

(1) (a) Munson, M. S. B. *J. Am. Chem. Soc.* **1965**, *87*, 2332. (b) Brauman, J. I.; Blair, L. K. *Ibid.* **1968**, *90*, 6561.

(2) Aue, D. H.; Webb, H. M.; Bowers, M. T. *J. Am. Chem. Soc.* **1973**, *95*, 2699.

(3) Taft, R. W.; Wolf, J. F.; Beauchamp, J. L.; Scorrano, G.; Arnett, E. M. *J. Am. Chem. Soc.* **1978**, *100*, 1240.

(4) Aue, D. H.; Bowers, M. T. "Gas Phase Ion Chemistry"; Bowers, M. T., Ed.; Academic Press: New York, 1979; Vol. 2, 78.

(5) (a) Shirley, D. A.; Martin, R. L. *J. Am. Chem. Soc.* **1974**, *96*, 5299. (b) Rabalais, W.; Davis, D. W. *Ibid.* **1974**, *96*, 5305.

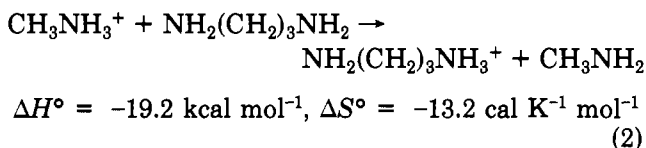
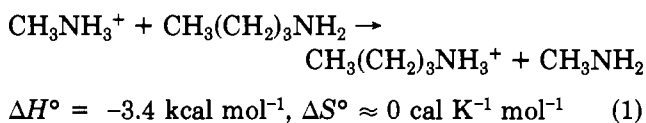
(6) Benoit, F. M.; Harrison, A. G. *J. Am. Chem. Soc.* **1978**, *100*, 3980.

The effects of primary structural factors were reviewed recently.<sup>4</sup>

Primary structural factors also affect substantially the interactions of complex ions with neutral molecules. From measurements on dimer ions,  $\text{B}_1\text{H}^+\text{B}_2$ , Kebarle concluded that the formation of the hydrogen bond involves partial proton transfer between  $\text{B}_1\text{H}^+$  and  $\text{B}_2$ , i.e., the bond  $\text{B}_1\text{—H}^+$  stretches as a partial  $\text{B}_2\cdots\text{H}^+$  bond forms. This transfer, in turn, is more efficient as the proton affinity difference  $\Delta\text{PA} = \text{PA}(\text{B}_2) - \text{PA}(\text{B}_1)$  decreases.<sup>7,8</sup> Indeed a recent examination<sup>9</sup> of over 120 dimers revealed inverse linear correlations between the dimer dissociation energies  $\Delta H^\circ_{\text{D}}$  and  $\Delta\text{PA}$  of the form  $\Delta H^\circ_{\text{D}} = C - b\Delta\text{PA}$  for the dimer types  $-\text{NH}^+\cdots\text{O}-$ ,  $-\text{NH}^+\cdots\text{N}-$ ,  $-\text{OH}^+\cdots\text{O}-$ ,  $-\text{NH}^+\cdots\text{S}-$ , and  $-\text{SH}^+\cdots\text{O}-$ .  $C$  and  $b$  are constants depending on the dimer type, for all types, the slope  $b$  is  $\approx 0.3 \pm 0.04$ . These relations apply over  $\Delta\text{PA}$  ranges as wide as 0–70 kcal mol<sup>-1</sup>. Further, for larger clusters of structurally simple ions  $\text{BH}^+$ , such as  $\text{BH}^+\cdots n\text{H}_2\text{O}$  ( $n = 2\text{--}4$ ), the ratio of multiple to single clustering energies  $\Delta H^\circ_{0,n}/\Delta H^\circ_{0,1}$  turned out to be constant, regardless of the identity of  $\text{BH}^+$ . These relations allow empirical prediction of ion–neutral interaction energies in hydrogen-bonding systems of structurally simple ions. More quantitative theoretical studies dealt with the geometry and charge-density changes in the vicinity of the ionic hydrogen bond,<sup>10–12</sup> which may be termed as primary structure effects on ion–neutral interactions.

### Intramolecular Hydrogen Bonding

When multiple functional groups are present in an ion, such as in  $\text{X}(\text{CH}_2)_n\text{YH}^+$ , an intramolecular hydrogen bond can form between  $\text{YH}^+$  and  $\text{X}$ . The significance of this structural factor becomes evident<sup>4,7,12</sup> when one considers the thermochemistry of two proton-transfer reactions:



The first reaction is exothermic since the proton affinity of the larger, more polarizable amine,  $\text{CH}_3(\text{CH}_2)_3\text{NH}_2$ , is higher than of methylamine. The entropy change for this reaction, which involves no significant structural changes, is negligible.

The polarizability of diaminopropane is similar to that of butylamine, and, considering only primary ef-

(7) Yamdagni, R.; Kebarle, P. *J. Am. Chem. Soc.* **1973**, *95*, 3504.

(8) (a) Hiraoka, K.; Grimsrud, E. P.; Kebarle, P. *J. Am. Chem. Soc.* **1974**, *96*, 3359. (b) Davidson, W. R.; Sunner, J.; Kebarle, P. *Ibid.* **1979**, *101*, 1675. (c) Kebarle, P. *Ann. Rev. Phys. Chem.* **1977**, *28*, 445 and references therein.

(9) Meot-Ner (Mautner), M. 31st Annual Conference, American Society for Mass Spectrometry, Boston, MA, 1983; *J. Am. Chem. Soc.* **1984**, *106*, 1257, 1265.

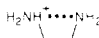
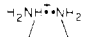
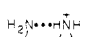
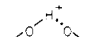
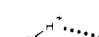
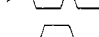
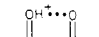
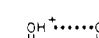
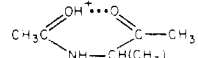
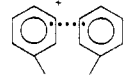
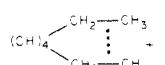
(10) Desmuelles, P. J.; Allen, L. C. *J. Chem. Phys.* **1980**, *72*, 4731.

(11) (a) Hiraoka, K.; Yamabe, S.; Sano, M. *J. Phys. Chem.* **1982**, *86*, 2626.

(b) Hiraoka, K.; Sano, M.; Yamabe, S. *Chem. Phys. Lett.* **1982**, *87*, 181.

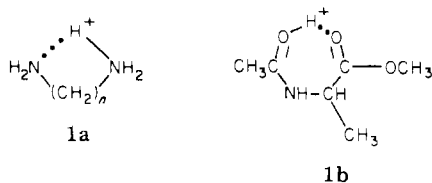
(12) (a) Meot-Ner (Mautner), M.; Hamlet, P.; Hunter, E. P.; Field, F. H. *J. Am. Chem. Soc.* **1980**, *102*, 6393. (b) Meot-Ner (Mautner), M. *Ibid.* **1984**, *106*, 278.

Table I  
 Thermochemical Parameters of Internal Hydrogen Bonds

compd	$-\Delta H^\circ_{\text{IHB}}^a$	$-S^\circ_{\text{IHB}}^b$	$-\Delta H^\circ_{\text{BWF}}^a$	$-\Delta S^\circ_{\text{IHB}}/n^b$
amines <sup>c</sup>				
	7	8	17	2.6
	14	15	9	3.7
	17	15	6	3.7
ethers <sup>d</sup>				
	7	4	23	1.4
	30	19	0	3.2
	18	3	12	
diketones <sup>d</sup>				
	2	4	28	2.0
	6	7	24	2.3
amino acid derivative <sup>e</sup>				
	7	14		4.6
intramolecular charge transfer complexes <sup>f</sup>				
	7	7	12	1.4
	≈ 3	7		1.4

<sup>a</sup> All values in kcal mol<sup>-1</sup>. <sup>b</sup> All values in cal mol<sup>-1</sup> K<sup>-1</sup>. <sup>c</sup> Reference 12a. <sup>d</sup> Reference 14. <sup>e</sup> Reference 12b. <sup>f</sup> Reference 15.

fects, reaction 2 should resemble reaction 1. However, reaction 2 is substantially more exothermic than reaction 1, which indicates further stabilization of the product diammonium ion in reaction 2, due to the formation of an intramolecular hydrogen bond (IHB)<sup>4,12,13</sup> (ion 1a). The large entropy change in reaction 2 can also be assigned mostly to the formation of the constrained ion (except for a small correction due to symmetry changes). The large entropy loss is due to the loss of several degrees of freedom upon the formation of the cyclic structure.



The difference  $\Delta H^\circ_2 - \Delta H^\circ_1$  yields the enthalpy of the internal hydrogen bond,  $\Delta H^\circ_{\text{IHB}}$ , and similarly,  $\Delta S^\circ_2 - \Delta S^\circ_1$  yields  $\Delta S^\circ_{\text{IHB}}$ . Similar comparisons between poly- and monofunctional ions yield the values shown in Table I. IHB enthalpy and entropy effects were first quantitatively measured in diamines by Yamdagni and

(13) Aue, D. H.; Webb, H. M.; Bowers, M. T. *J. Am. Chem. Soc.* **1973**, *95*, 2699.

Kebarle<sup>7</sup> and have been further measured in our laboratories in polyamines,<sup>12</sup> amino alcohols,<sup>12</sup> polyethers,<sup>14</sup> diketones,<sup>14</sup> and diphenylalkanes.<sup>15</sup> IHB enthalpy effects have also been observed in protonated fluoroacetone<sup>16</sup> and in transient intermediates in ion decomposition.<sup>17</sup> Recently, we obtained the IHB effect in the amino acid derivative  $\text{CH}_3\text{CO-Ala-OCH}_3\text{H}^+$ , where the geometry is similar to ionic hydrogen bonding between adjacent peptide links (ion 1b).<sup>12b</sup>

Since IHB effects are strongly structure dependent (Table I), further structure-related parameters are needed to characterize the intramolecular bond. The parameters that we employ are as follows.

(a) **Thermochemical values**,  $-\Delta H^\circ_{\text{IHB}}$  and  $-\Delta S^\circ_{\text{IHB}}$  as defined above.

(b) **Thermal stability of IHB**, as measured by the temperature  $T_{\text{op}}$ , required to open the IHB in half the ion population. At  $T_{\text{op}}$  and  $\Delta G^\circ_{\text{IHB}} = \Delta H^\circ_{\text{IHB}} - T\Delta S^\circ_{\text{IHB}} = 0$ ; therefore,  $T_{\text{op}} = \Delta H^\circ_{\text{IHB}}/\Delta S^\circ_{\text{IHB}}$ . For

(14) Meot-Ner (Mautner), M. *J. Am. Chem. Soc.* **1983**, *105*, 4906.

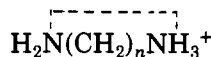
(15) Meot-Ner (Mautner), M.; Sieck, L. W. *J. Am. Chem. Soc.* **1981**, *103*, 5342.

(16) Drummond, D. F.; McMahon, T. B. *J. Phys. Chem.* **1981**, *85*, 3746.

(17) Bierman, H. W.; Morton, T. H. 30th Annual Conference on Mass Spectrometry, American Society for Mass Spectrometry, 1982, Proceeding, p 249.

most IHBs,  $T_{op}$  ranges from 500 to 2000 K; therefore, the intramolecular hydrogen bonds are usually stable at temperatures where the ions themselves are stable against pyrolysis.

(c) **Bond Weakening Factors.** Constraints imposed by the molecular structure can distend and angularly distort the hydrogen bond from its optimal geometry. These factors, combined with strain and intramolecular polarization weaken the intramolecular bond, compared with the hydrogen bond strength in an unconstrained dimer ion. The bond weakening factor, BWF, is therefore evaluated by comparing  $\Delta H^\circ_{IHB}$  in a polyfunctional ion, e.g.



with  $\Delta H^\circ_D$  of an analogous dimer, e.g.,  $\text{CH}_3\text{NH}^+\cdots\text{NH}_2\text{CH}_3$ .

(d) **Entropy Change.** The formation of the internal bond incorporates single bonds into a cyclic structure. Internal rotations about the bonds are transformed into vibrational modes, whose frequencies increase with the rigidity of the cyclic structure. A measure of the rigidity of the cyclic structures is given by the entropy change per single bond incorporated into the hydrogen bonded ring, i.e.,  $-\Delta S^\circ_{IHB}/n$ .

The experimental results show that  $\Delta H^\circ_{BWF}$  is high and  $-\Delta S^\circ_{IHB}/n$  is small in the difunctional ethanes (Table I), indicating a weak bond and loose structure when the ring is small. With increasing chain length,  $\Delta H^\circ_{BWF}$  decreases and  $-\Delta S^\circ_{IHB}/n$  increases as the bond optimizes and the structure tightens. Both in terms of larger  $\Delta H^\circ_{BWF}$  and smaller  $-\Delta S^\circ_{IHB}/n$  terms, the IHB in polyethers seems less efficient than in polyamines.

The exceptionally weak bonds and loose structure in  $\text{X}(\text{CH}_2)_2\text{XH}^+$  indicates that in the small ions the cyclic structure 1 may not be permanent. Rather, it may be only a preferred conformation stabilized by the "hydrogen bond". Rotation or loose libration about the C-C bond may still be possible;  $\Delta H^\circ_{IHB}$  constitutes only a barrier to rotation away from this favored conformation. This situation may be defined as a *partial hydrogen bond*. These weak bonds may be purely electrostatic, as was demonstrated by Houriet et al.<sup>20</sup> in cyclic  $\beta$ -amino alcohols, where the geometry is fixed and  $\Delta H^\circ_{IHB}$  is quantitatively determined by the Coulombic interactions between  $\text{NH}^+$  and the O-H dipole.

Intramolecular bonding can occur also in radical ions. Thus, the 1,4-diphenylbutane ion is stabilized by about 6 kcal mol<sup>-1</sup> due to the formation of intramolecular charge-transfer complexes (Table I). More surprisingly, the radical ions of unsubstituted C<sub>7</sub> and larger normal alkanes also seem to contain<sup>21</sup> "intramolecular dimers", resulting in negative entropies of ionization, up to -14 cal mol<sup>-1</sup> K<sup>-1</sup>.

### Interaction between Internal Hydrogen Bonding and External Solvation

When an internally hydrogen bonded ion is solvated (2), the charge is delocalized onto the solvent molecules.

(18) These values are obtained from a thermochemical cycle involving the  $k$ -fold solvation of the polyfunctional and a model monofunctional ion. The latter is a model for the solvation of the open form of the polyfunctional ion only at the  $-\text{NH}_3^+$  group.

(19) Kebarle, P., private communication.

(20) Houriet, R., submitted for publication.

(21) Meot-Ner (Mautner), M.; Sieck, L. W.; Ausloos, P. *J. Am. Chem. Soc.* 1981, 103, 5342.

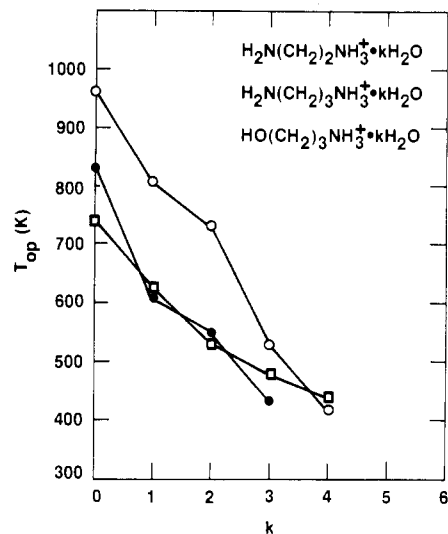
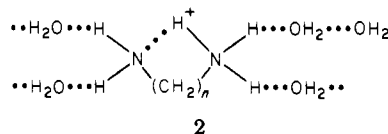


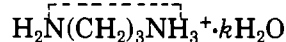
Figure 1. The effects of external hydration on the stability of intramolecular hydrogen bonds in  $\text{NH}_2(\text{CH}_2)_3\text{NH}_3^+ \cdot k\text{H}_2\text{O}$  (○),  $\text{NH}_2(\text{CH}_2)_2\text{NH}_3^+ \cdot k\text{H}_2\text{O}$  (●), and  $\text{HO}(\text{CH}_2)_3\text{NH}_3^+ \cdot k\text{H}_2\text{O}$  (□).

Solvation can therefore weaken and, in the extreme cases, displace the IHB.



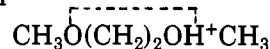
A value that reflects the effect of solvation on the stability of the IHB is  $(T_{op})_k$ , i.e., the thermal stability of the internal hydrogen bond in the  $k$ -fold solvated ion.  $(T_{op})_k$  is found from  $(\Delta H^\circ_{IHB}/\Delta S^\circ_{IHB})_k$  where  $(\Delta H^\circ_{IHB})_k$  and  $(\Delta S^\circ_{IHB})_k$  are the enthalpy and entropy changes of intramolecular hydrogen bond formation in the  $k$ -fold solvated ion.<sup>18</sup>

The values of  $(T_{op})_k$  fall rapidly with increasing  $k$  as shown in Figure 1, due to a combination of enthalpy and entropy effects. Solvation by only four  $\text{H}_2\text{O}$  molecules lowers the temperature required to open the hydrogen bond in



from 970 to 420 K.<sup>12</sup> A few more  $\text{H}_2\text{O}$  molecules may suffice to open the bond even at room temperature. In Figure 1 we therefore observe the gradual transition from a typical gas-phase property, intramolecular hydrogen bonding, to the typical condensed-phase phenomenon, the displacement of IHB by the external solvent.

A labile IHB can be displaced by a single solvent molecule. Thermochemistry indicates that this happens in monohydration and dimerization<sup>19</sup> of the small protonated diether

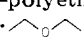
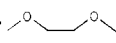
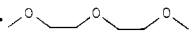
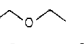
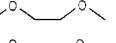
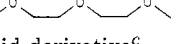


where the internal hydrogen bond is strained.

While external solvation weakens the internal hydrogen bond, the converse is also true; internal bonding can weaken or prevent interaction with external solvents. The effect is prominent in diethers, where internal bonding of the only  $-\text{OH}^+$  proton can completely block hydration or clustering under moderate conditions.<sup>22</sup>

(22) Morton, T. H.; Beauchamp, J. L. *J. Am. Chem. Soc.* 1972, 94, 3671.

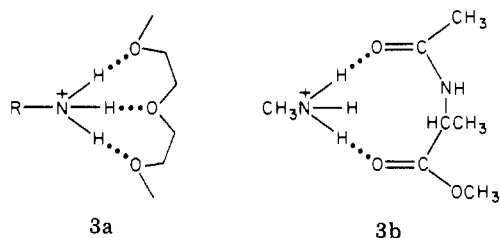
Table II  
Thermochemical Effects of Multiple Hydrogen Bonding<sup>a</sup>

	$\Delta H^\circ_D$	$\Delta S^\circ_D$	$\Delta H^\circ_{\text{multiple bonding}}$
amineH <sup>+</sup> -polyether <sup>b</sup>			
$c\text{-C}_6\text{H}_{11}\text{NH}_3^+$ · 	21.9	31.9	0
$c\text{-C}_6\text{H}_{11}\text{NH}_3^+$ · 	29.4	35.5	8
$c\text{-C}_6\text{H}_{11}\text{NH}_3^+$ · 	39.7	44.6	15
$c\text{-C}_6\text{H}_{11}\text{NH}_3^+$ · 18-crown-6	46	38	21
(CH <sub>3</sub> ) <sub>3</sub> NH <sub>3</sub> <sup>+</sup> · 	19.5	29.4	0
(CH <sub>3</sub> ) <sub>3</sub> NH <sub>3</sub> <sup>+</sup> · 	26.7	34.8	7
(CH <sub>3</sub> ) <sub>3</sub> NH <sub>3</sub> <sup>+</sup> · 	32.8	40.0	10
amino acid derivative <sup>c</sup> CH <sub>3</sub> NH <sub>3</sub> <sup>+</sup> · CH <sub>3</sub> CO-Ala-OCH <sub>3</sub>	40.1	35.1	12
nucleic bases <sup>d</sup>			
pyridine <sub>2</sub> H <sup>+</sup>	23.7	28	0
adenine <sub>2</sub> H <sup>+</sup>	30.3	39	7
cytosine <sub>2</sub> H <sup>+</sup>	38.3	37	15

<sup>a</sup>  $\Delta H$  in kcal mol<sup>-1</sup>;  $\Delta S$  in cal mol<sup>-1</sup> K<sup>-1</sup>. <sup>b</sup> Reference 23. <sup>c</sup> Reference 12b. <sup>d</sup> Reference 25.

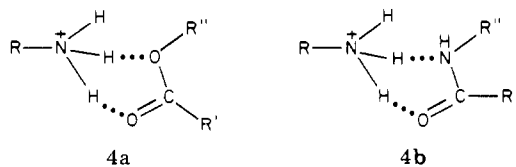
### Multiple Hydrogen Bonding

Multiple polar functional groups with lone-pair electrons enable a neutral molecule to form multiple hydrogen bonds with a protonated ion, thus stabilizing the ion-molecule complex. The effect is evident in ammonium ion-polyether complexes in the gas phase.<sup>23</sup> The magnitude of multiple bonding (MB) effects is revealed if one compares the dissociation energies of an RNH<sub>3</sub><sup>+</sup>-polyether complex (3a) with an RNH<sub>3</sub><sup>+</sup>-monoether complex (Table II).



The addition of a second and third hydrogen bond in the diether, triether, and tetraether complex increases the dissociation enthalpy  $\Delta H^\circ_D$  significantly. The RNH<sub>3</sub><sup>+</sup>-tetraether complex is the most strongly bound hydrogen-bonded complex observed so far. The large entropy changes associated with the formation of the complexes of open-chain polyethers reflect the loss of internal rotors in the multiply bonded structure. Evidence for multiple bonding is also found in the complex of CH<sub>3</sub>NH<sub>3</sub><sup>+</sup> with the peptide analogue CH<sub>3</sub>CO-Ala-OCH<sub>3</sub> (3b).

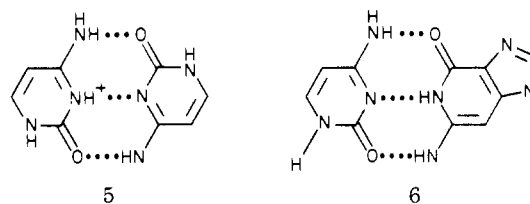
Other instances of multiple hydrogen bonding are observed in complexes of ammonium ions with large, highly polarizable esters and also with amides (4a, 4b).



The second bond stabilizes these dimers by 6–8 kcal mol<sup>-1</sup>, and the freezing of the rotation about the first

H bond, due to the formation of the second, increases the value of the entropy of dissociation  $\Delta S^\circ_D$  by 6–10 cal mol<sup>-1</sup> K<sup>-1</sup>.

The multiply bonded structures 3 and 4 involve the interaction of polydentate ligands with a single protonated group. A different type of multiple bonding, interactions between separate pairs of functional groups as shown in 5, seems to occur in dimer ions of nucleic



bases<sup>25</sup> (Table II). Again, the increased  $\Delta S^\circ_D$  of the nucleic base dimers vs. the pyridine dimers indicates that the formation of a second bond eliminates the free rotation about the -HN<sup>+</sup>...N- bond. The increased  $\Delta H^\circ_D$  shows that the second hydrogen bond in (adenine)<sub>2</sub>H<sup>+</sup> a further increase of 8 kcal mol<sup>-1</sup> occurs, which suggests a triply hydrogen bonded structure such as 5. The proposed configuration of hydrogen bonds in (adenine)<sub>2</sub>H<sup>+</sup> is exactly analogous to the adenine-thymine pair in DNA. Similarly, bonding in the proposed (cytosine)<sub>2</sub>H<sup>+</sup> dimer 5 is analogous to the cytosine-guanine pair in DNA 6.

### -C-H<sup>δ+</sup>...O- Hydrogen Bonds

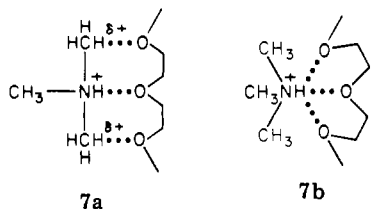
The stabilities of -NH<sub>3</sub><sup>+</sup>...polyether complexes reflect the effects of multiple -NH<sup>+</sup>...O- hydrogen bonds, as discussed above. To further explore multiple interactions in the ammonium ion-polyether complexes, we blocked two hydrogen bonds by using (CH<sub>3</sub>)<sub>3</sub>NH<sup>+</sup> instead of the primary ammonium ions RNH<sub>3</sub><sup>+</sup>. Surprisingly, substantial multiple bonding effects are still observed with polydentate ligands (Table II). Since in these complexes only one -NH<sup>+</sup>...O- hydrogen bond is possible, the further bonding may be ascribed to hydrogen bonding to the partially charged methyl hydrogens, i.e., -CH<sup>δ+</sup>...O- interactions (structure 7a).

(23) Meot-Ner (Mautner), *M. J. Am. Chem. Soc.* 1983, 105, 4912.

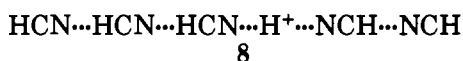
(24) Grimsrud, E. P.; Kebarle, P. *J. Am. Chem. Soc.* 1973, 7939.

(25) Meot-Ner (Mautner), *M. J. Am. Chem. Soc.* 1979, 101, 2396.

Alternatively, multiple interactions of the polar ether groups with one  $\text{-NH}^+$  group may occur (7b). However, the second such interaction is already as weak as a  $\text{-CH}^{\delta+}\cdots\text{O-}$  bond,<sup>11b</sup> and further interactions may be significantly weaker.



Other precedents for  $\text{-CH}^{\delta+}\cdots\text{X}$  bonds were seen by Grimsrud and Kebarle<sup>24</sup> in the trimer  $(\text{CH}_3)_2\text{OH}^+\cdots\text{O-}(\text{CH}_3)_2$ . As the only  $\text{-OH}^+$  function is already blocked in the dimer, the third molecule may add through a  $\text{-C-H}^{\delta+}\cdots\text{O-}$  bond, whose strength is  $10.1 \text{ kcal mol}^{-1}$ . Analogous  $\text{-C-H}^{\delta+}\cdots\text{N-}$  bonds are observed in the gas-phase ion cluster 8. Similar interactions were observed



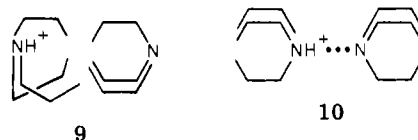
in the acetonitrile trimer.<sup>26</sup>  $\text{-C-H}^{\delta+}\cdots\text{O}$  hydrogen bonds have been suggested also by theoretical calculations and by crystallographic results.<sup>4,10,27,28</sup>

Direct evidence for significant  $\text{CH}^{\delta+}\cdots\text{X}$  interactions is provided by complexes of quaternary ammonium ions where only such interactions are possible. We observed complexes of  $(\text{CH}_3)_3\text{N}^+\text{CH}_3$  with one and two  $\text{H}_2\text{O}$  molecules ( $\Delta H^\circ_{0,1} = 9.0$ ,  $\Delta H^\circ_{1,2} = 9.4$ ), with one to three  $(\text{CH}_3)_2\text{CO}$  molecules ( $\Delta H^\circ_{0,1} = 14.6$ ;  $\Delta H^\circ_{1,2} = 13.0$ ;  $\Delta H^\circ_{2,3} = 11.7 \text{ kcal mol}^{-1}$ ), and similar complexes with other nitrogen and oxygen ligands, as well as with polydentate ligands, where multiple  $\text{CH}^{\delta+}\cdots\text{O}$  interactions yield total bonding energies up to  $23 \text{ kcal mol}^{-1}$ . Such interactions may model the bonding of acetylcholine,  $(\text{CH}_3)_3\text{N}^+\text{CH}_2\text{CH}_2\text{OCOCH}_3$ , with neuroreceptors.

### Steric Hindrance

The significance of a further structural effect, steric hindrance, was indicated by the observation that hindrance to ion solvation reduces substantially the aqueous basicity of 2,6-di-*tert*-butylpyridine.<sup>29</sup> Smaller effects are also observed in other 2-alkyl- and 2,6-di-alkylpyridines.<sup>30</sup> Steric effects also seem to decrease the equilibrium constants for dimerization of large alkylammonium ions.<sup>31</sup>

With relation to these steric effects, molecular models indicate that in all the ions the alkyl substituents can be so oriented as to prevent the  $\text{-NH}^+\cdots\text{N-}$  configuration from assuming optimal hydrogen bonding geometry. In the larger amines, the alkyl chains can completely block bonding (9). Distortion or blocking of the hydrogen bond would then weaken the bonding—an enthalpy effect. On the other hand, in all cases, even in the most hindered dimers, the substituents can be so oriented as to permit optimal hydrogen bonding



geometry (10). However, this requires constraining the rotational freedom of the alkyl groups and also of the rotation about the hydrogen bond—an entropy effect. These observations pose the question: is steric hindrance to ion-neutral interactions in those dimers primarily an enthalpy or entropy effect?

The experimental results for the dimer ions of alkylpyridines,<sup>30</sup> amines,<sup>30</sup> and ethers<sup>9</sup> provide a clear answer:  $\Delta H^\circ_D$  remains constant within each series, despite increasingly bulky substitution. Thus,  $\Delta H^\circ_D$  for dimers from the unhindered (4-methylpyridine)<sub>2</sub>H<sup>+</sup> to dimers of 2-*tert*-butyl-, 2,6-diethyl-, and 2,6-diisopropylpyridineH<sup>+</sup> is constant at  $23 \pm 1 \text{ kcal mol}^{-1}$ . However, the entropies of association become substantially more negative with hindrance, from  $-27.8$  to  $-39.8$ ,  $-37.4$ , and  $-48.1 \text{ cal mol}^{-1} \text{ K}^{-1}$ , respectively. Similarly, the enthalpies remain constant at  $-23 \pm 1 \text{ kcal mol}^{-1}$ , but entropies vary from  $-32.0$  to  $-56.5 \text{ cal mol}^{-1} \text{ K}^{-1}$  in  $(\text{R}_3\text{N})_2\text{H}^+$  dimers from  $\text{R} = \text{CH}_3$  to  $\text{R} = n\text{-C}_4\text{H}_9$ . Further, in hydration by one water molecule, i.e., in the formation of  $\text{BH}^+\cdots\text{H}_2\text{O}$  dimers, steric hindrance results in a substantial entropy effect. An especially large effect ( $-41 \text{ cal mol}^{-1}$ ) is observed in 2,6-di-*tert*-butylpyridineH<sup>+</sup>, where association with one water molecule freezes the rotations of both *tert*-butyl groups as well as of  $\text{H}_2\text{O}$ .

Observations similar to the above were also made in (ether)<sub>2</sub>H<sup>+</sup> dimers from  $((\text{CH}_3)_2\text{O})_2\text{H}^+$  to  $((n\text{-C}_6\text{H}_{11})_2\text{O})_2\text{H}^+$ .<sup>9</sup> Only in  $((i\text{-C}_3\text{H}_7)_2\text{O})_2\text{H}^+$ , where models show that optimal H bonding geometry may be prevented<sup>32</sup> was a small steric enthalpy effect observed.

The observations on steric hindrance may be summarized as follows. As long as there exists a conformation that allows optimal hydrogen bonding, steric hindrance does not weaken the bond, even if in most other conformations the bond is blocked. However, steric hindrance results in substantial entropy losses due to the loss of internal rotational freedom in the dimers.

### Charge Delocalization in Extended $\pi$ Systems

We now turn to another type of organic ions, radical ions of planar polycyclic aromatic hydrocarbons, and other structural features, increasing molecular size and conjugated  $\pi$  systems. From benzene to naphthalene, anthracene, and higher polycyclic aromatics, the ionization potentials (IPs) decrease and the proton affinities increase with increasing molecular size (Table III).<sup>33</sup> From the IP and PA, the homolytic bond dissociation energy  $D(\text{B}^+\text{-H})$  can be obtained from the relation:


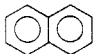
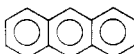
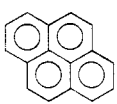

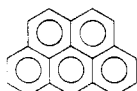
$$D(\text{B}^+\text{-H}) = \text{PA}(\text{B}) + \text{IP}(\text{B}) - \text{IP}(\text{H}) = \Delta H^\circ_f(\text{B}^+) - \Delta H^\circ_f(\text{BH}^+) + \Delta H^\circ_f(\text{H}) \quad (3)$$

According to (3),  $D(\text{B}^+\text{-H})$  reflects the difference between the stability of the radical ion  $\text{B}^+$  where both the charge and spin are delocalized in the large  $\pi$  system and of  $\text{BH}^+$  where only the charge is delocalized. With increasingly large  $\pi$  systems,  $D(\text{B}^+\text{-H})$  first decreases due to increasing spin delocalization; but once the spin

(26) Meot-Ner (Mautner), M. *J. Am. Chem. Soc.* **1978**, *100*, 4694.  
 (27) DeBoer, J. A.; Reinhardt, D. N.; Harkema, S.; van Hummel, G. J.; de Jong, F. *J. Am. Chem. Soc.* **1982**, *104*, 4073.  
 (28) Taylor, R.; Kennard, O. *J. Am. Chem. Soc.* **1982**, *104*, 5063.  
 (29) Aue, D. H.; Webb, H. M.; Bowers, M. T.; Liotta, C. L.; Alexander, C. J.; Hopkins, H. P. *J. Am. Chem. Soc.* **1976**, *98*, 854.  
 (30) Meot-Ner (Mautner), M.; Sieck, L. W. *J. Am. Chem. Soc.* **1983**, *105*, 2956.  
 (31) Kroeger, M. K.; Drago, R. S. *J. Am. Chem. Soc.* **1981**, *103*, 3250.

(32) Larsen, J. W.; McMahon, T. B. *J. Am. Soc.* **1982**, *104*, 6255.  
 (33) Meot-Ner (Mautner), M. *J. Phys. Chem.* **1980**, *84*, 2716.

Table III  
 Thermochemistry of Ionization, Protonation of Polycyclic Aromatics, and Dimerization of the Ions<sup>a</sup>

compd	IP	PA <sup>e</sup>	$\Delta H^\circ_{D^+}$ (B <sup>+</sup> -H)	$\Delta H^\circ_{D^+}$ (BH <sup>+</sup> ·B)	$\Delta H^\circ_{D^+}$ (B <sup>+</sup> ·B)	$\Delta H^\circ_{\text{resonance}}{}^b$	$-\Delta H^\circ_{\text{pol}}{}^c$	$-\Delta H^\circ_{\text{LJ}}{}^d$
	222.5	181.3	81	11.0	17.0	6.0	7.1	3.5
	187.7	194.3	68	14.1	17.8	3.7	6.4	8.2
	171.9	207.4	66	16.0	16.4	0.4	4.4	13.1
	173.0	206.5	66	16.5	19.1	2.6		
	167.4	208.6	62	21.4	21.6	0.2		
	170.8	205.0	62		23.8			

<sup>a</sup> All values in kcal mol<sup>-1</sup>, from ref 35 and 36. <sup>b</sup> Charge resonance terms, from  $\Delta H^\circ_{\text{resonance}} = -\Delta H^\circ_{D^+}(\text{B}_2^+) - \Delta H^\circ_{D^+}(\text{B}_2\text{H}^+)$ .  
<sup>c</sup> Electrostatic ion-induced dipole interactions. <sup>d</sup> Lennard-Jones type dispersion interactions. <sup>e</sup> Referred to PA(NH<sub>3</sub>) = 205 kcal mol<sup>-1</sup>.

is extensively delocalized, D(B<sup>+</sup>-H) levels off to a constant value of 62 ± 2 kcal mol<sup>-1</sup> in the largest ions, even though PA and IP keep changing in a compensating manner.

### Resonance Charge Transfer in Ionic Complexes

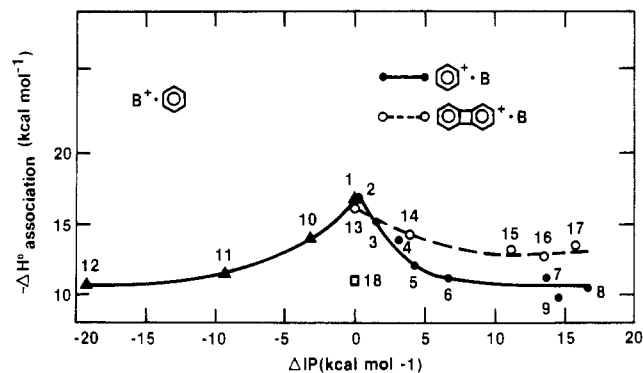
We now turn to intermolecular interactions, first in the radical dimer ions B<sub>1</sub><sup>+</sup>·B<sub>2</sub>.<sup>34-36</sup> The most simple ion in this series is the benzene dimer ion, where the two resonance structures C<sub>6</sub>H<sub>6</sub><sup>+</sup>·C<sub>6</sub>H<sub>6</sub> ↔ C<sub>6</sub>H<sub>6</sub>·C<sub>6</sub>H<sub>6</sub><sup>+</sup> are of equal energy and  $\Delta H^\circ_{\text{resonance}}$  can be significant. The contribution of  $\Delta H^\circ_{\text{resonance}}$  should then decrease in mixed dimers where the charge would be localized on the component with the lower IP. When the difference between the IPs of B<sub>1</sub> and B<sub>2</sub>, i.e.,  $\Delta\text{IP}$ , is large,  $\Delta H^\circ_{\text{resonance}}$  should vanish and only electrostatic interactions would remain. Indeed,  $\Delta H^\circ_{D^+}$  decreases asymptotically with increasing  $\Delta\text{IP}$ , from 17 kcal mol<sup>-1</sup> in (C<sub>6</sub>H<sub>6</sub>)<sub>2</sub><sup>+</sup> to about 11 kcal mol<sup>-1</sup> in C<sub>6</sub>H<sub>6</sub><sup>+</sup>·C<sub>6</sub>F<sub>6</sub> (Figure 2). The difference, 6 kcal mol<sup>-1</sup>, can be ascribed to  $\Delta H^\circ_{\text{resonance}}$ . The limiting value of  $\Delta H^\circ_{D^+}$ , 11 kcal mol<sup>-1</sup>, is the same as the bonding interaction in the protonated dimer C<sub>6</sub>H<sub>7</sub><sup>+</sup>·C<sub>6</sub>H<sub>6</sub>, where charge resonance is also absent. Indeed, we can use the difference between radical and protonated dimers,  $\Delta H^\circ_{D^+}(\text{B}^+\cdot\text{B}) - \Delta H^\circ_{D^+}(\text{BH}^+\cdot\text{B})$ , to evaluate  $\Delta H^\circ_{\text{resonance}}$  in a series of dimers of polycyclic aromatics.

When such studies were applied to radical dimers of PAHs of increasing size,<sup>36</sup> it was found that  $\Delta H^\circ_{\text{resonance}}$  falls off rapidly in the larger dimers (Table III). Apparently, charge delocalization in the large  $\pi$  system of the monomer makes charge delocalization to an external electron donor less favorable.

(34) Field, F. H.; Hamlet, P.; Libby, W. F. *J. Am. Chem. Soc.* 1967, 89, 6035.

(35) Meot-Ner (Mautner), M.; Hamlet, P.; Hunter, E. P.; Field, F. H. *J. Am. Chem. Soc.* 1978, 100, 5466.

(36) Meot-Ner (Mautner), M. *J. Phys. Chem.* 1980, 84, 2724.



**Figure 2.**  $\Delta H^\circ_{D^+}$  of radical dimer ions as a function of the difference between the ionization potentials of the components ( $\Delta\text{IP}$ ), in three sets of dimers. Set I (●): benzene<sup>+</sup>·B, where B is (1) benzene, (2) 2-fluoro-, (3) 1,2-difluoro-, (4) 1,3-difluoro-, (5) 1,2,4,5-tetrafluoro-, (6) 1,2,3,5-tetrafluoro-, (7) pentafluoro-, (8) hexafluorobenzene, (9) cyclohexane. Set II (▲): B<sup>+</sup>·benzene, where B<sup>+</sup> is (10) chlorobenzene<sup>+</sup>, (11) toluene<sup>+</sup>, (12) 1,3,5-trimethylbenzene<sup>+</sup>. Set III (○): Biphenylene<sup>+</sup>·B, where B is (13) biphenylene, (14) acenaphthylene, (15) benzoindene, (16) naphthalene, (17) biphenylene and (18) (□) represents the benzene H<sup>+</sup>-benzene dimer. Note that the difference between the maximum and the asymptotic limit is 6 kcal mol<sup>-1</sup> in the benzene series but only 3 ± 1 kcal mol<sup>-1</sup> in the biphenylene series, which indicates  $\Delta H^\circ_{\text{resonance}} = 6$  kcal mol<sup>-1</sup> in benzene<sub>2</sub><sup>+</sup> but only 3 kcal mol<sup>-1</sup> in biphenylene<sub>2</sub><sup>+</sup>.

Further, calculations show that intermolecular electrostatic, ion-induced dipole forces also fall off with increasing charge dispersion in the large ions.<sup>36</sup> Therefore, theoretical arguments as well as experimental evidence show that all ionic intermolecular interactions decrease with increasing molecular size both in the radical and protonated dimer ions.

### Attractive van der Waals Dispersion Forces

The conclusion just reached would suggest that  $\Delta H^\circ_{D^+}$  should decrease in the larger dimers. Therefore, it was



surprising that  $\Delta H^\circ_D$  actually increases and exceeds 20 kcal mol<sup>-1</sup> in the largest dimers (Table III).

The reason for this trend is clarified by Lennard-Jones type calculations on intermolecular interactions.<sup>36</sup> We observe (Table III) that while in (benzene)<sub>2</sub><sup>+</sup> the polarization and resonance interactions are dominant, already in (naphthalene)<sub>2</sub><sup>+</sup> dispersion forces become the dominant bonding term. Evidently, even as the ionic forces decrease with increasing size, the increasing number of interacting carbon centers in these sandwich type dimers makes the dispersion forces dominant.

#### Implications for Condensed-Phase Chemistry

The trends observed with increasing molecular size in the properties of polycyclic aromatic hydrocarbons may be extrapolated to the largest member of the series, i.e., graphite. Using the IP and PA data we calculated the bond dissociation energies  $D^\circ(B^+-H)$ . We found that  $D^\circ(B^+-H)$  first decreases and then levels off at  $62 \pm 2$  kcal mol<sup>-1</sup> in the larger six- to eight-membered ring compounds, where, apparently, the stabilizing effect of spin delocalization has reached its limit. Further increase in molecular size, up to graphite, is therefore not expected to change this value significantly. Using the value of  $D^\circ(\text{graphite}^+-H) = 62$  kcal mol<sup>-1</sup> and eq 5 yields PA(graphite) 276 kcal mol<sup>-1</sup> for edge protonation of a single graphite layer.<sup>36</sup> Interestingly, this is nearly identical with the proton affinity of bulk water.<sup>37</sup> Considering entropy effects, a graphite layer should be a stronger base than bulk water, at least with respect to the addition of a single proton.

Using the observations on PAH dimer ions, we can speculate about the properties of a graphite crystal. As we saw, with increasing size intermolecular ionic forces between components of the polycyclic aromatic dimer ions decrease and vanish. Therefore, in the largest dimers, i.e., two adjacent graphite layers, ionic interactions will not stabilize the ionized layer. Therefore, we conclude that the IP and PA of a graphite crystal should be equal to that of a single graphite layer, i.e., 101 and 277 kcal mol<sup>-1</sup>, respectively.

As another example of extrapolation from gas-phase to condensed-phase chemistry, we can draw an inference from the results on amineH<sup>+</sup>-polyether complexes upon the energetics of enzyme-catalyzed H<sup>+</sup>-transfer reactions. In enzymes, polar groups provide an environment resembling crown ether,<sup>38</sup> which stabilize an ionic intermediate such as  $-\text{NH}_3^+ \cdots -\text{OOC}-$ . To compete with aqueous environments, the strength of the enzyme-intermediate interactions must be over 70 kcal mol<sup>-1</sup>.<sup>38</sup> However, we find that the enthalpy of even optimal  $-\text{NH}_3^+ \cdots$  crown interactions is less than 50 kcal mol<sup>-1</sup>. Therefore, other interactions such as  $-\text{NH}_3^+ \cdots$  ionic groups, or  $-\text{COO}^- \cdots$  polar groups, must provide

additional stabilization in the enzyme to exceed ion solvation in water.

The potential importance of ionic hydrogen bonding in biological intermediates is also suggested by the protonation and complexes of CH<sub>3</sub>CO-Ala-OCH<sub>3</sub>, which suggest intramolecular and multiple IHB interactions of peptide amide links, up to 30 kcal mol<sup>-1</sup>/bond.

#### Concluding Remarks

Structural complexity results in thermochemical effects that indicate the following interactions:

**Intramolecular hydrogen bonding** in a variety of protonated polyfunctional amines, ketones, and ethers stabilizes the ions up to 30 kcal mol<sup>-1</sup>. Such effects were also observed in a dipeptide analogue. The thermochemistry of protonated polypeptides should be investigated, since intramolecular hydrogen bonding in protonated biopolymers may be significant in reactions proceeding through ionic intermediates.

**Multiple hydrogen bonding** is indicated in dimers and complexes involving polyfunctional ions and ligands. However, data is available for less than 20 complexes and more is needed to investigate the effects of structural variation. Especially interesting are the indications for CH<sup>δ+</sup>...X bonding, which can be further explored in complexes such as R<sub>3</sub>NCH<sub>3</sub><sup>+</sup>...X<sup>-</sup>, where only such bonds are possible.

**Steric hindrance** leads to substantial entropy, but not enthalpy, effects in complexes where at least one conformation allows the hydrogen bond length to be optimized. Of interest would be ionic hydrogen bond strengths in even more severely hindered complexes where steric hindrance distends the bond. From such complexes one could deduce the functional relation between XH<sup>+</sup>...Y bond length and the strength of the ionic hydrogen bond.

**Resonance charge transfer** stabilizes aromatic radical dimer ions by up to 6 kcal mol<sup>-1</sup>. With increasing intramolecular charge delocalization the intermolecular ionic interactions vanish. However, in large ions attractive dispersion forces become significant. Thermochemical equilibrium measurements have dealt so far only with π donor-π acceptor complexes. The thermochemical effects in charge-transfer complexes of n donor-n acceptor and mixed n-π donor and acceptor systems will be of interest.

Gas-phase thermochemical data on structurally complex ions is still scarce; the above structural factors were studied in less than 100 ions and complexes. Interactions involving further structural factors and combinations thereof will be of interest. Such phenomena are often observed in larger, nonvolatile molecules. Such studies will benefit from further applications of direct-probe PHPMS and temperature-controlled ICR studies and data from the photoionization of van der Waals clusters.

(37) Klotz, C. E. *J. Phys. Chem.* 1981, 85, 3585.

(38) Warshel, A. *Acc. Chem. Res.* 1981, 14, 284.